Physics - Informed Machine Learning for Reduced Space Chemical Kinetics

Anuj Kumar
Mechanical and Aerospace Engineering
North Carolina State University
Raleigh, NC 27695
akumar35@ncsu.edu

Tarek Echekki
Mechanical and Aerospace Engineering
North Carolina State University
Raleigh, NC 27695
techekk@ncsu.edu

Abstract

Modeling detailed chemical kinetics stands as a primary challenge in combustion simulations. Recent machine learning (ML) approaches aim to accelerate chemical kinetics integration, though their application is often limited to simpler reaction mechanisms. This study presents a novel framework to enforce physical constraints, specifically total mass and elemental conservation, into the training of ML models for reduced-space chemical kinetics of large and complex reaction mechanisms. Given the strong correlation between full and reduced solution vectors, our method utilizes a small neural network to establish an accurate and physically consistent mapping. By leveraging this mapping, we enforce physical constraints in the training process of the ML model for reduced space chemical kinetics. The framework is demonstrated here with the chemical kinetics of CH_4 oxidation. The resulting solution vectors from our Deep Operator Networks-based approach are not only accurate but also align more consistently with physical laws.

1 Introduction

The detailed modeling of chemical kinetics is the principal bottleneck in the combustion simulations. Recently, several efforts have been made to learn the chemical kinetics and accelerate its integration in a simulation using Machine Learning (ML) tools (1; 2; 3; 4; 5). However, due to the rapid increase in the dimensionality of the governing ODE system as the chemical reaction mechanisms become more complex, the machine learning models have predominantly been restricted to simpler mechanisms. For larger and more complex reaction mechanisms that have a high-dimensional solution vector of thermochemical scalars, chemical kinetics is learned in the reduced space (6; 7; 8), either through dimensionality reduction techniques (9; 10) or by selecting a set of representative species (5; 11). While ML models have demonstrated significant potential in capturing chemical kinetics in the reduced space, the temporal evolution of the reduced solution vector may not conform to certain physical constraints, like total mass and elemental conservation. These physical constraints are typically essential for a CFD solver, potentially hindering the integration of the machine learning model with such a solver. Recent efforts have explored incorporating domain-specific physical principles or laws into neural network training by adjusting the loss function (12), allowing the models to not only rely on data but also on established physical knowledge. An obvious step of incorporating the physical constraint of total mass and elemental conservation in the training process of the machine learning model for reduced space chemical kinetics is hindered by the unavailability of the full solution vector. Enforcing these physical constraints in the training process often requires access to the full solution vector. In this paper, we introduce a framework that enables the integration of physical constraints into the training process of machine learning models on reduced-space chemical kinetics. This framework is readily adaptable to any machine learning model aiming to capture kinetics or dynamics in a reduced space. The framework relies on the strong correlation

Machine Learning and the Physical Sciences Workshop, NeurIPS 2023.

between full and reduced solution vectors, establishing a high-fidelity and physically consistent mapping from the reduced set to the full set using a small neural network. Leveraging this high-fidelity and physically consistent mapping, the primary training process for identifying chemical kinetics in reduced space can enforce physical constrain with an apparent access to the full solution. The framework is demonstrated on the chemical kinetics of CH_4 oxidation. To capture the chemical kinetics, we adopt the framework of Kumar and Echekki (8), based on Deep Operator Networks (DeepONets) (13), which accurately learns the chemical kinetics operator in the reduced space of representative thermochemical scalars. We first establish an accurate and physically consistent mapping from the reduced set to the full solution vector. Subsequently, we successfully incorporate the physical constraints of total mass and elemental conservation into the training of DeepONet, which learns chemical kinetics in a reduced space. As a result, the solution vector produced by DeepONet achieves greater physical consistency retaining its predictive accuracy.

2 Methodology

2.1 Chemical-Kinetics identification through a Deep Operator Network

For a 0D, homogeneous and constant-pressure reactor, temperature and species are evolved based on a system of ODEs, which are solved as an initial value problem taking the form:

$$\frac{d\phi_i}{dt} = f(\phi, p_0), \quad i = 1, 2, 3, \ldots, n \quad \text{and} \quad \phi(0) = \phi_0 \tag{1}$$

where ϕ is the thermochemical composition vector, which includes species mass fractions and temperature. The term, $f(\phi, p_0)$ is a function of thermochemical scalars, ϕ, and represents the chemical reaction source terms based on the law of mass action. Chemical kinetics presented by the above system of stiff ODEs is learnt through a DeepONet framework of Kumar and Echekki (8), where a set of representative species, as a reduced set $\in R^m$, is considered instead of a full thermochemical solution vector $\in R^n$. The dimensionality of reduced space (R^m) is far smaller than the dimensionality of the original solution vector (R^n). In order to train the DeepONet, as shown in Figure -1a, a reduced solution set at any instant in time ($\phi(t)$) inputs to the Branch Net and the time-step ($\delta t \in (0, \Delta t)$) by which the solution needs to be advanced inputs to the Trunk Net and the output of the DeepONet is minimized against the corresponding advanced solution vector ($\phi(t + \delta t)$) such that loss is given by:

$$\mathcal{L}_{\text{DATA}} = \frac{1}{m} \sum_{i=1}^{m} \left(\phi_i(t + \delta t) - \phi_i^*(t + \delta t)\right)^2 \tag{2}$$

where δt varies from 0 to a large fixed time-step (Δt) and $\phi_i^*(t+\delta t)$ is the corresponding ground-truth value.

2.2 Mapping left-out scalars from reduced set: Correlation Net

Although the dimensionality of full solution vector is very large, it lives on a low dimensional manifold since most of the scalars are highly correlated (14; 15). The reduced set ($\phi_i, i = 1, 2, \ldots m$), identified based on principal component analysis of reaction rate data as mentioned in Alqahtani and Echekki (16), is representative of the thermochemical manifold and it is highly correlated to the left out scalars ($\phi_i, i = m + 1, m + 2, \ldots n$). Leveraging the high correlation, left-out scalars can be mapped from the reduced set through an ANN denoted as Correlation Net as shown in Figure-1b. Inputs and outputs to the Correlation Net are reduced set and left-out scalars respectively as shown in Figure-1b and the corresponding loss is:

$$\mathcal{L}_{\text{C-DATA}} = \frac{1}{(m - n)} \sum_{i=m+1}^{n} \left(\phi_i - \phi_i^*\right)^2 \tag{3}$$

Since the full thermochemical space obeys certain physical laws, such as the sum of species mass-fractions is one and elements remain conserved during the reaction as the solution vector evolves, Correlation Net can be trained with additional losses corresponding to these physical constraints.

$$\mathcal{L}_{\text{C-SUM-MF}} = \left| \sum_{i=1}^{n} \phi_i - 1.0 \right| \quad \text{and} \quad \mathcal{L}_{\text{C-ELEM}} = \sum_{K=1}^{N_{\text{Element}}} \left| \sum_{i=1}^{n} \frac{N_K^i W_K}{W_i} (\phi_i - \phi_i^*) \right| \tag{4}$$

where N_K^i is the K^{th} element contribution in i^{th} species and W_K is the atomic weight of K^{th} element and W_i is the molecular weight of the i^{th} species. It should be noted that these two losses not just include Correlation Net output but also its input. The total loss function for Correlation Net takes this form:

$$\mathcal{L}_C = W_1 \mathcal{L}_{\text{C-DATA}} + W_2 \mathcal{L}_{\text{C-SUM-MF}} + W_3 \mathcal{L}_{\text{C-ELEM}} \tag{5}$$

Where W_1, W_2 and W_3 are the weights for each loss term.

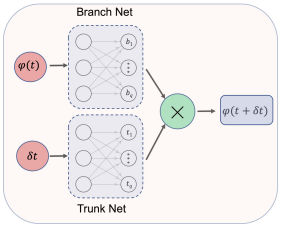

(a) DeepONet for chemical kinetics identification in reduced space

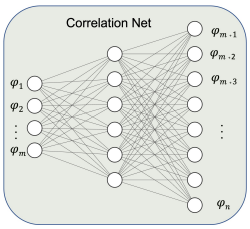

(b) Mapping of left-out scalars from reduced Set

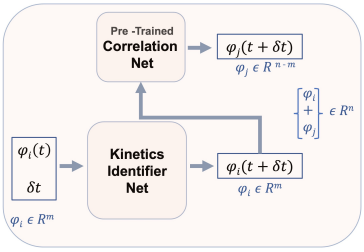

(c) Full solution sector from reduced space chemical kinetics

Figure 1: Framework of physics - informed machine learning in the reduced space chemical kinetics

2.3 Physics-constrained chemical kinetics identification

As mentioned, the chemical kinetics for any reaction system is identified through a DeepONet in the reduced space. For any reduced solution vector, the left-out solution vector can be reconstructed through the pre-trained Correlation Net. Apparently, the mapping from Correlation Net extends the reduced set to the full solution vector as shown in Figure-1c. Utilizing the mapping provided by pre-trained Correlation Net, the training process of DeepONet, as mentioned in Section-2.1, can now be enriched with the physical constraints of species and elemental mass conservation, as formulated in Section-1b, with the corresponding losses defined here:

$$\mathcal{L}_{\text{SUM-MF}} = \left| \sum_{i=1}^{n} \phi_i(t + \delta t) - 1.0 \right| \tag{6}$$

$$\mathcal{L}_{\text{ELEM}} = \sum_{K=1}^{N_{\text{Element}}} \left| \sum_{i=1}^{n} \frac{N_K^i W_K}{W_i} \left(\phi_i(t + \delta t) - \phi_i^*(t + \delta t) \right) \right| \tag{7}$$

in addition to the data loss that is defined as:

$$\mathcal{L}_{\text{DATA}} = \frac{1}{m} \sum_{i=1}^{m} \left(\phi_i(t + \delta t) - \phi_i^*(t + \delta t) \right)^2 \tag{8}$$

The total loss becomes:

$$\mathcal{L} = W_1 \mathcal{L}_{\text{DATA}} + W_2 \mathcal{L}_{\text{SUM-MF}} + W_3 \mathcal{L}_{\text{ELEM}} \tag{9}$$

Where W_1, W_2 and W_3 are the weights for each loss term.

3 Results

The framework of training DeepONet with physical constraints in reduced space is demonstrated on 0D CH_4 oxidation. The solution profiles for training purposes are generated from Cantera (17) with GRI-MECH 3.0 (18) having 53 species and 325 reactions. The solution vector consisting of species mass fractions and temperature is evolved in time for initial temperatures of T_i = 1100, 1110, 1120, 1130, 1140 and 1150 K and equivalence ratios of Φ = 0.8, 0.9, 1.0, 1.1 and 1.2. Instead of the full thermochemical vector (54 scalars), the reduced set of 8 representative species (H_2, H_2O, CH_4, CO_2, CH_3OH, O_2, CO, NO) and Temperature are considered for the chemical kinetics learning through the DeepONet model. First, the Correlation Net is trained with the physical constraints on the full dataset where the reduced set and left-out scalars (reduced set removed from full solution vector) are input and output to the model respectively. Then, utilizing the mapping from the pre-trained Correlation Net, the DeepONet model is trained with the physical constraints for chemical kinetics identification. Both, Correlation Net and DeepONet, are modeled and trained with the JAX framework (19) on an NVIDIA A100 GPU with the Adamax optimizer (20). The size of trainable parameters of Correlation Net is 1100 and for DeepONet it is 55,000. Correlation Net and DeepONet are trained for 300,000 and 80,000 iterations taking around 3.3 minutes and 10.5 minutes, respectively, of GPU time. Weights for individual losses in the total loss formulation, W_1, W_2 and W_3 are 0.6, 0.2 and 0.2, respectively, for training of both Correlation Net and DeepONet.

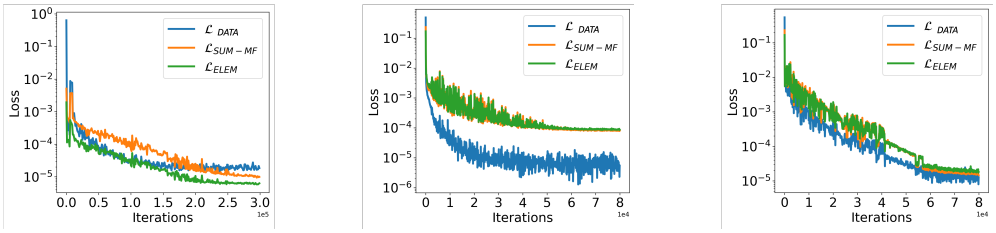

(a) (b) (c)

Figure 2: a) Correlation Net training loss decay with physical constraints of species and elemental mass conservation. b) DeepONet training loss decay without physical constraint. c) DeepONet training loss decay with physical constraint

Losses with and without physical constraints are shown in Figure-2. Physical constraints in the training process of Correlation Net and DeepONet further decrease the losses corresponding to the physical conservations. Prediction results from Correlation Net for a single time-series dataset are shown in Figure-3. It can be observed that, by imposing physical constraints in the model training, errors are reduced by an order of magnitude for total mass and elemental conservation keeping predictions accurate (MAE of around 7×10^{-5}).

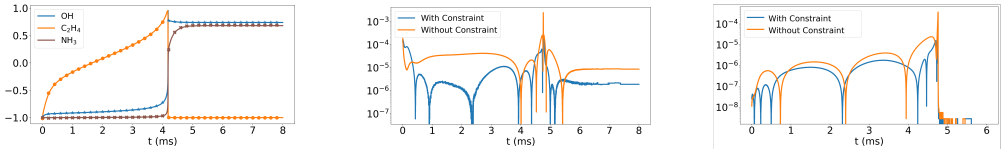

(a) Precise mapping of left-out scalars (b) Sum of mass-fraction error (c) 'C' element conservation error

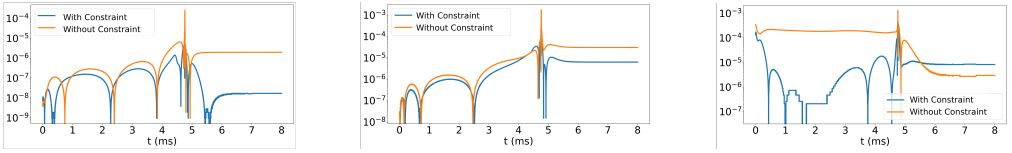

(d) 'H' element conservation error (e) 'O' element conservation error (f) 'N' element conservation error

Figure 3: Accurate and physically consistent mapping through Correlation Net. a) Accurate reconstruction of left-out scalars. b) The sum of mass-fraction error is lower with physical constraint. c-f) With physical constraints, lower elemental conservation error for 'C', 'H', 'O', and 'N' respectively.

Predictions evolved from DeepONet for a particular initial condition (T_i=1150K, Φ = 1.1) are shown in Figure-4. It can be observed that, by imposing physical constraints in the model training, errors are reduced by an order of magnitude for total mass and elemental conservation keeping accurate predictions of chemical kinetics (MAE of around 5×10^{-3}.)

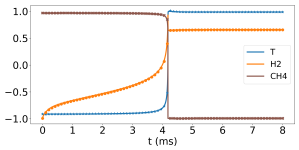

(a) Accurate evolution of solutions

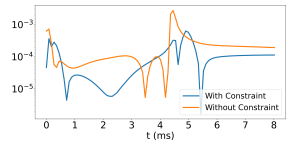

(b) Sum of mass-fraction error

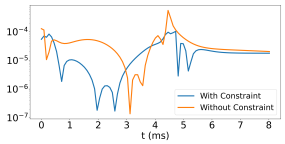

(c) 'C' element conservation error

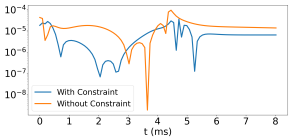

(d) 'H' element conservation error

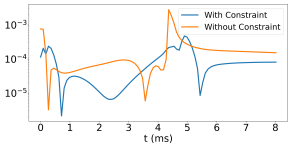

(e) 'O' element conservation error

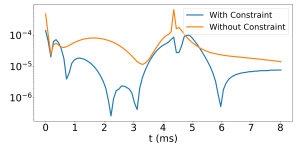

(f) 'N' element conservation error

Figure 4: Accurate and physically consistent predictions from DeepONet for chemical kinetics. a) Accurate predictions of the solution vector. b) The sum of mass-fraction error is lower with physical constraint. c-f) With physical constraints, lower elemental conservation error for 'C', 'H', 'O', and 'N' respectively.

4 Conclusion and Future Works

The proposed framework facilitates the enforcement of physical constraints in the training process of an ML model for reduced space chemical kinetics of large and complex reaction mechanisms. Utilizing this, the evolved solution vector corresponding to CH_4 oxidation, based on DeepONets, aligns more consistently with physical laws maintaining the prediction accuracy. In the future, the approach will be extended to even larger and more complex reaction mechanisms. Additionally, the loss associated with the governing stiff ODE will also be integrated into the ML training process.

Acknowledgments and Disclosure of Funding

This research was funded by Saudi Aramco through a contract number ASC Agreement No. CW47993. This research used resources of the National Energy Research Scientific Computing Center (NERSC), a U.S. Department of Energy Office of Science User Facility located at Lawrence Berkeley National Laboratory, operated under Contract No. DE-AC02-05CH11231 using NERSC award BES-ERCAP0020203.

References

[1] J. Blasco, N. Fueyo, C. Dopazo, and J. Ballester, "Modelling the temporal evolution of a reduced combustion chemical system with an artificial neural network," *Combustion and Flame*, vol. 113, no. 1, pp. 38–52, 1998. [Online]. Available: https://www.sciencedirect.com/science/article/pii/S0010218097002113

[2] R. Ranade, S. Alqahtani, A. Farooq, and T. Echekki, "An ann based hybrid chemistry framework for complex fuels," *Fuel*, vol. 241, pp. 625–636, 04 2019.

[3] C. D. J Blasco, N Fueyo and J.-Y. Chen, "A self-organizing-map approach to chemistry representation in combustion applications," *Combustion Theory and Modelling*, vol. 4, no. 1, pp. 61–76, 2000.

[4] W. Ji and S. Deng, "Autonomous discovery of unknown reaction pathways from data by chemical reaction neural network," *The Journal of Physical Chemistry A*, vol. 125, no. 4, pp. 1082–1092, 2021.

[5] M. Haghshenas, P. Mitra, N. D. Santo, and D. P. Schmidt, "Acceleration of chemical kinetics computation with the learned intelligent tabulation (LIT) method," *Energies*, vol. 14, no. 23, 2021. [Online]. Available: https://www.mdpi.com/1996-1073/14/23/7851

[6] H. E. Dikeman, H. Zhang, and S. Yang, *Stiffness-Reduced Neural ODE Models for Data-Driven Reduced-Order Modeling of Combustion Chemical Kinetics*. [Online]. Available: https://arc.aiaa.org/doi/abs/10.2514/6.2022-0226

[7] A. Kumar, M. Rieth, O. Owoyele, J. H. Chen, and T. Echekki, "Acceleration of turbulent combustion dns via principal component transport," *Combustion and Flame*, vol. 255, p. 112903, 2023. [Online]. Available: https://www.sciencedirect.com/science/article/pii/S0010218023002845

[8] A. Kumar and T. Echekki, "A Framework for Combustion Chemistry Acceleration with DeepONets," *arXiv preprint arXiv:2304.12188*, 2023. [Online]. Available: https://doi.org/10.48550/arXiv.2304.12188

[9] D. H. Ballard, "Modular learning in neural networks," in *Proceedings of the Sixth National Conference on Artificial Intelligence - Volume 1*, ser. AAAI'87. AAAI Press, 1987, p. 279–284.

[10] S. Wold, K. Esbensen, and P. Geladi, "Principal component analysis," *Chemometrics and Intelligent Laboratory Systems*, vol. 2, no. 1, pp. 37–52, 1987, proceedings of the Multivariate Statistical Workshop for Geologists and Geochemists. [Online]. Available: https://www.sciencedirect.com/science/article/pii/0169743987800849

[11] O. Owoyele and P. Pal, "Chemnode: A neural ordinary differential equations framework for efficient chemical kinetic solvers," *Energy and AI*, vol. 7, p. 100118, 2022. [Online]. Available: https://www.sciencedirect.com/science/article/pii/S2666546821000677

[12] M. Raissi, P. Perdikaris, and G. Karniadakis, "Physics-informed neural networks: A deep learning framework for solving forward and inverse problems involving nonlinear partial differential equations," *Journal of Computational Physics*, vol. 378, pp. 686–707, 2019. [Online]. Available: https://www.sciencedirect.com/science/article/pii/S0021999118307125

[13] L. Lu, P. Jin, G. Pang, Z. Zhang, and G. E. Karniadakis, "Learning nonlinear operators via deeponet based on the universal approximation theorem of operators," *Nature Machine Intelligence*, vol. 3, no. 3, pp. 218–229, 2021. [Online]. Available: https://doi.org/10.1038/s42256-021-00302-5

[14] S. B. Pope, "Small scales, many species and the manifold challenges of turbulent combustion," *Proceedings of the Combustion Institute*, vol. 34, no. 1, pp. 1–31, 2013. [Online]. Available: https://www.sciencedirect.com/science/article/pii/S1540748912003963

[15] A. Coussement, B. J. Isaac, O. Gicquel, and A. Parente, "Assessment of different chemistry reduction methods based on principal component analysis: Comparison of the mg-pca and score-pca approaches," *Combustion and Flame*, vol. 168, pp. 83–97, 2016. [Online]. Available: https://www.sciencedirect.com/science/article/pii/S0010218016300384

[16] S. Alqahtani and T. Echekki, "A data-based hybrid model for complex fuel chemistry acceleration at high temperatures," *Combustion and Flame*, vol. 223, pp. 142–152, 2021. [Online]. Available: https://www.sciencedirect.com/science/article/pii/S0010218020304065

[17] D. Goodwin, H. Moffat, and R. Speth, "Cantera: An object-oriented software toolkit for chemical kinetics, thermodynamics, and transport processes. version 2.2.0," 01 2015.

[18] M. Frenklach, H. Wang, M. Goldenberg, G. Smith, D. Golden, C. Bowman, R. Hanson, W. Gardiner, and V. Lissianski, "Gri-mech—an optimized detailed chemical reaction mechanism for methane combustion," 01 2000.

[19] R. Frostig, M. Johnson, and C. Leary, "Compiling machine learning programs via high-level tracing," 2018. [Online]. Available: https://mlsys.org/Conferences/doc/2018/146.pdf

[20] D. P. Kingma and J. Ba, "Adam: A method for stochastic optimization," *arXiv preprint arXiv:1412.6980*, 2014.